

AD-756 655

ALTITUDE-AIDED RADAR TRACKING

L. L. Goertzen

Pacific Missile Range

Prepared for:

Naval Air Systems Command

20 October 1972

DISTRIBUTED BY:

NTIS

National Technical Information Service
U. S. DEPARTMENT OF COMMERCE
5285 Port Royal Road, Springfield Va. 22151



AD 756655

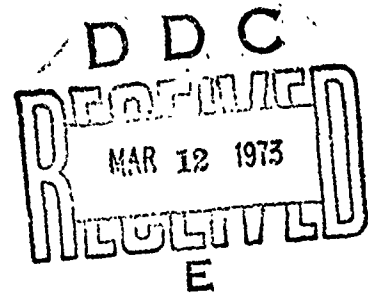
ALTITUDE-AIDED RADAR TRACKING

By

L. L. GOERTZEN
Mathematical and Engineering
Processes Division

20 October 1972

NATIONAL TECHNICAL
INFORMATION SERVICE
NATIONAL AERONAUTICS AND SPACE ADMINISTRATION
WASHINGTON, D.C. 20540



APPROVED FOR PUBLIC RELEASE; DISTRIBUTION UNLIMITED.



PACIFIC MISSILE RANGE

Point Mugu, California

PMR-TP-72-10 (U)

32

PACIFIC MISSILE RANGE

POINT MUGU, CALIFORNIA

W. M. HARNISH, RADM USN

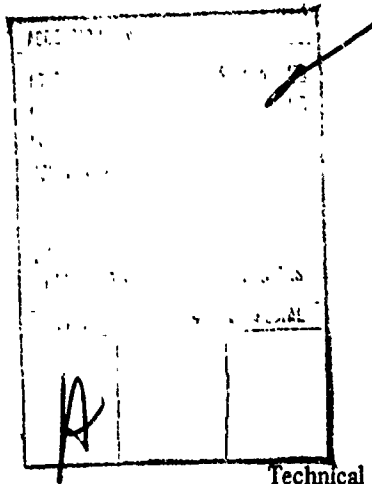
Commander

Mr. Sorrell Berman, Head, Math Analysis Branch; Mr. C. L. Tubbs, Head, Math and Engineering Processes Division; and Mr. J. F. Donlan, Head, Scientific Data Analysis and Processing Department, have reviewed this report for publication.

Approved by:

W. L. MILLER

Technical Director



Technical Publication PMR-TP-72-10

Published by Editing and Writing Branch

Technical Publications Division

Photo/Graphics Department

Security classification UNCLASSIFIED

First printing 60 copies

UNCLASSIFIED

Security Classification

DOCUMENT CONTROL DATA - R & D

(Security classification of title, body of abstract and indexing annotation must be entered when the overall report is classified)

1. ORIGINATING ACTIVITY (Corporate author) Pacific Missile Range Point Mugu, California 93042		2a. REPORT SECURITY CLASSIFICATION UNCLASSIFIED	
		2b. GROUP	
3. REPORT TITLE ALTITUDE-AIDED RADAR TRACKING			
4. DESCRIPTIVE NOTES (Type of report and inclusive dates)			
5. AUTHOR(S) (First name, middle initial, last name) L. L. Goertzen			
6. REPORT DATE 20 October 1972		7a. TOTAL NO. OF PAGES 32	7b. NO. OF REFS 4
8a. CONTRACT OR GRANT NO.		9a. ORIGINATOR'S REPORT NUMBER(S) PMR-TP-72-10	
b. PROJECT NO.		9b. OTHER REPORT NO(S) (Any other numbers that may be assigned this report)	
c.			
d.			
10. DISTRIBUTION STATEMENT Approved for Public release; distribution unlimited.			
11. SUPPLEMENTARY NOTES		12. SPONSORING MILITARY ACTIVITY Naval Air Systems Command	
13. ABSTRACT <p>This report describes an algorithm that is used to determine the maximum likelihood position of an aircraft from the measurement of one radar's range, azimuth, and elevation and from an altitude measurement of the aircraft. The variances of these measurements must also be known.</p> <p>The report also shows how much the altitude-aided algorithm improves the accuracy as compared to a one-radar determination.</p> <p>It was concluded that:</p> <ol style="list-style-type: none">1. The position error in the low radar elevation angle ACMTS (Air Combat Maneuvering Test System) geometry at the Pacific Missile Range, obtained by using a telemetered altitude measurement and the R, A, and E from one radar in the algorithm described in the report, could be reduced from 1/2 to 1/5 that of the position error obtained when only the R, A, E measurement from one radar is used.2. The altitude measurement greatly reduces the error in determination of the position point when the aircraft being tracked is a large distance from the radar.			

DD FORM 1 NOV 65 1473 (PAGE 1)

S/N 0101-607-6801

UNCLASSIFIED

Security Classification

I-a

UNCLASSIFIED

Security Classification

14 KEY WORDS	LINK A		LINK B		LINK C	
	ROLE	WT	ROLE	WT	ROLE	WT
Altitude measurement Low elevation angle radar tracking improvement Maximum likelihood estimate Multivariate normal probability density function Radar measurement Random vector Real time application Tracking Variance-covariance matrix						

I-6

CONTENTS

	Page
SUMMARY	1
INTRODUCTION	3
METHOD	4
EFFECTS OF THE ALGORITHM AND IMPROVEMENT OF TRACKING DATA	9
CONCLUSIONS	10
REFERENCES	10
APPENDIX	
Flowcharts	25
FIGURES	
1. Example of a Geometric Situation Used to Determine Algorithm Effects and Improvement in Accuracy	11
2. Plots Showing the Effects of the Algorithm With Respect to Variances in the Elevation Measurement	12
3. Plot Showing the Increase in Precision of the Algorithm Over the Radar-Only Solution	15
4. Plot Showing the Increases in Position Accuracy as Range Increases	16
5. Plots Showing the Cartesian Coordinate That the Altitude Measure- ment Aids	17
6. Example of a Geometric Situation Used to Determine Improvement in Algorithm Accuracy	23

PACIFIC MISSILE RANGE
Point Mugu, California

ALTITUDE-AIDED RADAR TRACKING

By
L. L. GOERTZEN

SUMMARY

This report describes an algorithm that is used to determine the maximum likelihood position of an aircraft from the measurement of one radar's range, azimuth, and elevation and from an altitude measurement of the aircraft. The variances of these measurements must also be known.

The report also shows how much the altitude-aided algorithm improves the accuracy as compared to a one-radar determination.

It was concluded that:

1. The position error in the low radar elevation angle ACMTS (Air Combat Maneuvering Test System) geometry at the Pacific Missile Range, obtained by using a telemetered altitude measurement and the R, A, and E from one radar in the algorithm described in the report, could be reduced from 1/2 to 1/5 that of the position error obtained when only the R, A, E measurement from one radar is used.
2. The altitude measurement greatly reduces the error in determination of the position point when the aircraft being tracked is a large distance from the radar.

INTRODUCTION

This report describes an algorithm that is used to determine the maximum likelihood position of an aircraft from the measurements of range, azimuth, and elevation from one radar and from the altitude measurement of the aircraft. This algorithm, a direct application of information in reference 1, would be easy to extend to include data from several radars. However, this report is written with the ACMTS (Air Combat Maneuvering Test System) in mind. That system requires that from two to six aircraft be tracked simultaneously; hence it appears that the situation where more than one radar will track a single aircraft will seldom be realized.

In reference 2, recommendation is made to use a radar altitude-aided position determination algorithm that neglects the elevation measurement completely. Reference 2 rejected the method of weighting all the data according to anticipated accuracies because that type of method complicated the calculations and did not appear to offer a significant improvement in the accuracy of low-altitude measurements over the method which neglected the elevation measurement.

The maximum likelihood estimate may require more calculations to accomplish; specifically several more sine, cosine functions must be calculated. However, this procedure is not complicated and certainly is usable in real-time. The procedure outlined in this report has the following advantages over the technique which neglects the elevation angle measurement:

1. The elevation angle (even at small elevations) may be a better measurement than the altitude measurement. This depends upon the location of the aircraft with respect to the radar. For example, when the aircraft is less than 15 miles from the radar, the elevation angle measurement with a standard deviation of 0.5 degree is better than an altitude measurement with a standard deviation of 100 feet.
2. It is a good general purpose procedure. It can use combined altitude and elevation data when these measurements are of nearly equal accuracy.
3. It allows a continuous transition from inaccurate elevation angle data to accurate elevation angle data. When the accuracy of the elevation angle gains quality and should be used in the position solution, this algorithm does not have to be disregarded and a new procedure adopted. This algorithm provides a way to use accuracy evaluations of the elevation angle

data as an operation proceeds and to weight the elevation data accordingly in the position solution.

Reference 2 and the paragraphs of this report that describe the effects of the algorithm indicate that altitude-aided radar tracking greatly increases the accuracy over tracking that uses radar data alone. With the ACMTS, where altitude data from a telemetry source is available in the computer, it would be negligence if an altitude-aided radar tracking procedure were not included in the ACMTS software.

This report will proceed by first mathematically describing the algorithm; then the effects and improvements resulting from the algorithm will be shown by examining the following:

1. The influence of the altitude accuracy and altitude measurement in the maximum likelihood range, azimuth, and elevation as compared to the range, azimuth, and elevation of the radar alone.
2. The influence of the altitude accuracy on the accuracy of the maximum likelihood position estimate.
3. The determination of the slant ranges at which altitude-aided tracking gives significant increases in the accuracy of the position point.

METHOD

Suppose that one radar measures the position of an aircraft and that the altitude of the object above the earth is measured. It is desired to combine these measurements into an optimal position determination of the object.

It is assumed that

1. The radar measurement is independent of the altitude measurement, and
2. The probability density functions of the radar (f_R) and altitude (f_H) measurements are gaussian, i.e.,

$$f_R(R, A, E)$$

$$= \frac{1}{(2\pi)^{3/2}} \frac{1}{|M_R|^{1/2}} \exp \left(-\frac{1}{2} \begin{bmatrix} R - \mu_R & A - \mu_A & E - \mu_E \end{bmatrix} M_R^{-1} \begin{bmatrix} R - \mu_R \\ A - \mu_A \\ E - \mu_E \end{bmatrix} \right)$$

$$f_H(x, y, z)$$

$$= \frac{1}{(2\pi)^{3/2}} \frac{1}{|M_H|^{1/2}} \exp \left(-\frac{1}{2} \begin{bmatrix} x - \mu_x & y - \mu_y & z - \mu_z \end{bmatrix} M_H^{-1} \begin{bmatrix} x - \mu_x \\ y - \mu_y \\ z - \mu_z \end{bmatrix} \right)$$

where

(R, A, E) is the random vector representing the radar measurements

M_R is the variance-covariance matrix of (R, A, E)

(μ_R, μ_A, μ_E) is the mean of (R, A, E)

(x, y, z) is the random vector representing the altitude measurements

z is the altitude measurement

Since x and y are not measured, their variances are infinite

M_H is the variance-covariance matrix of (x, y, z)

(μ_x, μ_y, μ_z) is the mean of (x, y, z)

3. The spherical variance-covariance matrix, M_R , can be transformed to a Cartesian variance matrix by the linear map approximation of the first order Taylor Series.
4. The latitude and longitude of the location of the altitude measurement are known. This is a reasonable assumption since (R, A, E) measurements can be used to calculate this point and the variance in the altitude will be insensitive to small errors in the location of the altitude measurement.

M_R can be propagated to a Cartesian variance-covariance matrix, M_{RH} , referenced to the point on the earth where the altitude was measured, i.e.,

$$M_{RH} = T_2 T_3 M_R T_3^T T_2^T$$

where T_2 and T_3 are 3×3 matrices (see reference 3), and T_2^T and T_3^T are the transpositions of the matrices T_2 and T_3 .

$$T_3 (1, 1) = \cos E \sin A$$

$$T_3 (1, 2) = R \cos E \cos A$$

$$T_3 (1, 3) = -R \sin E \sin A$$

$$T_3 (2, 1) = \cos E \cos A$$

$$T_3 (2, 2) = -R \cos E \sin A$$

$$T_3 (2, 3) = -R \sin E \cos A$$

$$T_3 (3, 1) = \sin E$$

$$T_3(3, 2) = 0$$

$$T_3(3, 3) = R \cos E$$

$$T_2(1, 1) = \cos(\lambda_p - \lambda_r)$$

$$T_2(1, 2) = \sin \phi_r \sin(\lambda_p - \lambda_r)$$

$$T_2(1, 3) = -\cos \phi_r \sin(\lambda_p - \lambda_r)$$

$$T_2(2, 1) = -\sin \phi_p \sin(\lambda_p - \lambda_r)$$

$$T_2(2, 2) = \cos \phi_r \cos \phi_p + \sin \phi_r \sin \phi_p \cos(\lambda_p - \lambda_r)$$

$$T_2(2, 3) = \sin \phi_r \cos \phi_p - \cos \phi_r \sin \phi_p \cos(\lambda_p - \lambda_r)$$

$$T_2(3, 1) = \cos \phi_p \sin(\lambda_p - \lambda_r)$$

$$T_2(3, 2) = \cos \phi_r \sin \phi_p - \sin \phi_r \cos \phi_p \cos(\lambda_p - \lambda_r)$$

$$T_2(3, 3) = \sin \phi_r \sin \phi_p + \cos \phi_r \cos \phi_p \cos(\lambda_p - \lambda_r)$$

where ϕ_r and λ_r are the latitude and longitude of the origin of the radar and ϕ_p and λ_p are the latitude and longitude of the position of the aircraft.

The probability density function of the radar measurements in the Cartesian coordinate system whose origin is at the point on the earth where the altitude was measured is

$$f_{RC}(x_R, y_R, z_R) = \frac{1}{(2\pi)^{3/2}} \frac{1}{|M_{RH}|^{1/2}} \exp \left(-\frac{1}{2} [x_R - \mu_x, y_R - \mu_y, z_R - \mu_z] M_{RH}^{-1} \begin{bmatrix} x_R - \mu_x \\ y_R - \mu_y \\ z_R - \mu_z \end{bmatrix} \right)$$

From assumption 1* the probability density function of x, y, z, x_R, y_R, z_R is

$$f_{RC} \cdot f_H = f(x, y, z, x_R, y_R, z_R)$$

* Radar measurement is independent of the altitude measurement.

$$= \frac{1}{(2\pi)^3} \frac{1}{|M_H|^{1/2}} \frac{1}{|M_{RH}|^{1/2}} \exp \left(-\frac{1}{2} \left([x-\mu_x, y-\mu_y, z-\mu_z] M_H^{-1} \begin{bmatrix} x-\mu_x \\ y-\mu_y \\ z-\mu_z \end{bmatrix} + [x_R-\mu_x, y_R-\mu_y, z_R-\mu_z] M_{RH}^{-1} \begin{bmatrix} x_R-\mu_x \\ y_R-\mu_y \\ z_R-\mu_z \end{bmatrix} \right) \right)$$

As in reference 1, pages 4 through 7, a mean (μ_x, μ_y, μ_z) is found such that for the probability density function f , the data point (x, y, z, x_R, y_R, z_R) is most likely to approximate (μ_x, μ_y, μ_z) .

Let

$$M_{RH}^{-1} = \begin{bmatrix} S_{11} & S_{12} & S_{13} \\ S_{21} & S_{22} & S_{23} \\ S_{31} & S_{32} & S_{33} \end{bmatrix}$$

$$M_H^{-1} = \begin{bmatrix} \frac{1}{\sigma_x^2} & 0 & 0 \\ 0 & \frac{1}{\sigma_y^2} & 0 \\ 0 & 0 & \frac{1}{\sigma_z^2} \end{bmatrix}$$

Now

$$M_H^{-1} \text{ becomes } \begin{bmatrix} 0 & 0 & 0 \\ 0 & 0 & 0 \\ 0 & 0 & \frac{1}{\sigma_z^2} \end{bmatrix}$$

since x and y are not measured; their variances are assumed to be infinite.

Now directly from reference 1

$$\begin{bmatrix} \mu_x \\ \mu_y \\ \mu_z \end{bmatrix} = \begin{bmatrix} c_1 & c_4 & c_5 \\ c_4 & c_2 & c_6 \\ c_5 & c_6 & c_3 \end{bmatrix}^{-1} \begin{bmatrix} c_7 \\ c_8 \\ c_9 \end{bmatrix}$$

where

$$c_1 = S_{11}$$

$$c_2 = S_{22}$$

$$c_3 = S_{33} + \frac{1}{\sigma_z^2}$$

$$c_4 = S_{12}$$

$$c_5 = S_{13}$$

$$c_6 = S_{23}$$

$$c_7 = S_{11} x_R + S_{12} y_R + S_{13} z_R$$

$$c_8 = S_{12} x_R + S_{22} y_R + S_{23} z_R$$

$$c_9 = S_{13} x_R + S_{23} y_R + S_{33} z_R + \frac{z}{\sigma_z^2}$$

The variance-covariance matrix of (μ_x, μ_y, μ_z) is

$$\begin{bmatrix} c_1 & c_4 & c_5 \\ c_4 & c_2 & c_6 \\ c_5 & c_6 & c_3 \end{bmatrix}^{-1}$$

See the appendix for logical flow and arrangement of the equations presented into a computer program.

EFFECTS OF THE ALGORITHM AND IMPROVEMENT OF TRACKING DATA

The geometrical situation diagramed in figure 1 was used in the generation of figures 2 and 3. It is assumed that the radar measures an aircraft at $(R, A, E) = (50 \text{ nautical miles}, 20 \text{ degrees}, 10 \text{ degrees})$ when the altitude measurement on the aircraft is 1 nautical mile. These two measurements were made inconsistent purposely so that it can be observed how the algorithm solution converges to the radar solution as the variance in the altitude measurement increases. If the radar were making a consistent measurement to the altitude of 1 nautical mile, the elevation angle, E , would be approximately 0.7 degree.

Figure 2 compares the algorithm's determination of R , A , and E respectively to the R , A , and E of radar measurements. Figure 2 also shows how the algorithm converges to the radar measurements as the variance in the altitude measurement increases, as well as how the altitude measurement and its accuracy affect the range, azimuth, and elevation estimates. The symbols 1, 2, and 3 in figure 2 represent different standard deviations in the elevation angle: 1 assumes a $\sigma_E = 10 \text{ mils}$, 2 assumes $\sigma_E = 1 \text{ mil}$, and 3 assumes $\sigma_E = 0.1 \text{ mil}$. The standard deviations of range and azimuth of the radar measurements are held constant at 10 feet and 0.1 mil.

Figure 3 shows how position error* of the algorithm converges to the position error of radar measurement as the uncertainty in the altitude increases. The increase in accuracy of the algorithm with respect to the radar-only measurement as a function of altitude variance is shown also. The symbols 1, 2, and 3 in figure 3 represent σ_E 's of 10 mils, 1 mil, and 0.1 mil where σ_R equals 10 feet and σ_A equals 0.1 mil remain constant. The horizontal lines at position errors of 185.1 feet, 85.4 feet, and 39.6 feet indicate the position errors of the radar-only measurement for the respective standard deviations in elevations of 10 mils, 1 mil, and 0.1 mil.

Figure 4 shows how the altitude-aided radar tracking algorithm increases the position accuracy as compared to radar-only tracking. The symbol 1 in figure 4 describes the position error of the radar alone as a function of slant range, and the symbol 2 describes the position error of the altitude-aided radar position determination as a function of slant range. The following typical values for standard deviations in range, azimuth, elevation, and altitude were used in calculating figure 4: $\sigma_R = 20 \text{ feet}$, $\sigma_A = 0.2 \text{ mil}$, $\sigma_E = 0.2 \text{ mil}$, and $\sigma_H = 20 \text{ feet}$.

Figure 5 shows how the x , y , z rectangular radar components are affected by the altitude-aided radar tracking computations. An assumed trajectory of $z_i = 30,000 \text{ feet}$, $x_i = y_i = i(10,000) \text{ feet}$; $i = 1, 2, \dots, 200$ was converted to range, azimuth, elevation, and altitude parameters. (See figure 6.) Noise with a standard deviation of 20 feet was placed on range, 0.2 mil was placed on azimuth, 0.2 mil was placed on elevation, and 20 feet was placed on altitude. These noisy parameters were input into the altitude-aided tracking algorithm and the x , y , z outputs from the algorithm were differenced with the nominal x , y , z and plotted versus $i = 1, 2, \dots, 200$. The resulting plots are shown in figure 5, parts a, c, and e. To obtain comparisons to the radar-only position determination, the noisy range, azimuth, and elevation parameters were used to compute x , y , z

*Position error is defined as the radius of a sphere whose volume is that of the volume of the 69 percent probability ellipsoid. For discussions of probability ellipsoids see reference 4.

and these were differenced with the nominal x, y, z and plotted versus $i = 1, 2, \dots, 200$. The resulting plots are shown in figure 5, parts b, d, and f. Comparing the plots in figure 5 shows that the altitude-aided tracking technique has little effect on the precision of x and y but greatly increases the precision of z.

CONCLUSIONS

1. The position error in the low radar elevation angle ACMTS geometry at PMR obtained by using a telemetered altitude measurement and the R, A, and E from one radar in the maximum likelihood algorithm described in this report, could be reduced from 1/2 to 1/5 that of the position error obtained when only the R, A, and E measurement from one radar is used. The factors of 1/2 and 1/5 are obtained by using figure 3 and assuming the standard deviation in elevation is between 1 to 10 mils and the standard deviation in altitude is between 20 and 100 feet.
2. The altitude measurement greatly reduces the error in determination of the position point when the object being tracked is a large distance from the radar. (See figure 4 and figure 5 parts e and f.)
3. The position error reduction occurs in the components in which the altitude was measured. See figures 5 and 6.
4. Some altitude-aided radar tracking technique should be incorporated in the ACMTS real-time software. Two possibilities are:
 - a. The technique outlined in reference 2. Its advantage is the shortness of computations.
 - b. The technique outlined in this report. Its advantages are that it is more accurate than the technique outlined in reference 2 and is versatile in adjusting to changing accuracies in the measured data.

REFERENCES

1. Pacific Missile Range. N-Station Credibility Gap, by L. L. Goertzen. Point Mugu, Calif., PMR, Oct 1972. (Technical Publication PMR-TP-72-8) UNCLASSIFIED.
2. Stanford Research Institute. Radar Improvement Program for the Pacific Missile Range, Volume 1: Improved Low-Altitude Position Accuracy Using Combined Radar Altitude Measurements, by N. E. Owens and J. P. McHenry. Menlo Park, California, Aug 1969. (SRI Project 6600 Contract N00019-67-C-0411) UNCLASSIFIED.
3. Pacific Missile Range. Propagating Covariance Matrices of Radar Coordinates, by K. W. Jutzi. Point Mugu, Calif., PMR, Dec 1969. (Technical Note 3430-4-70) UNCLASSIFIED. (Available from Code 3430)
4. ----- Effects of Dimension-Reducing Mappings on Gaussian Probability Density Functions, by Lando Goertzen. Point Mugu, Calif., PMR, 18 Jul 1969. (PMR Technical Memorandum PMR-TM-69-3) UNCLASSIFIED.

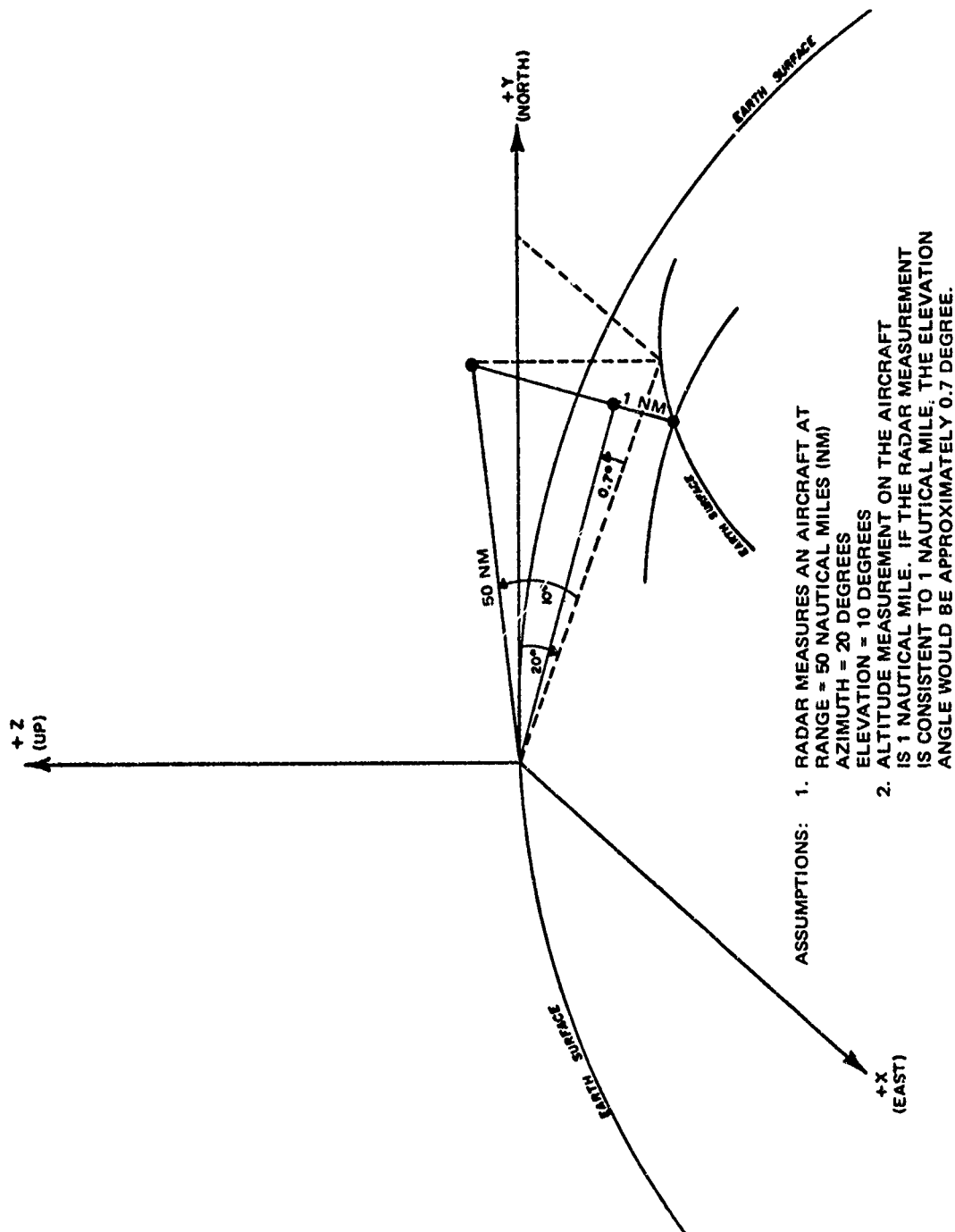
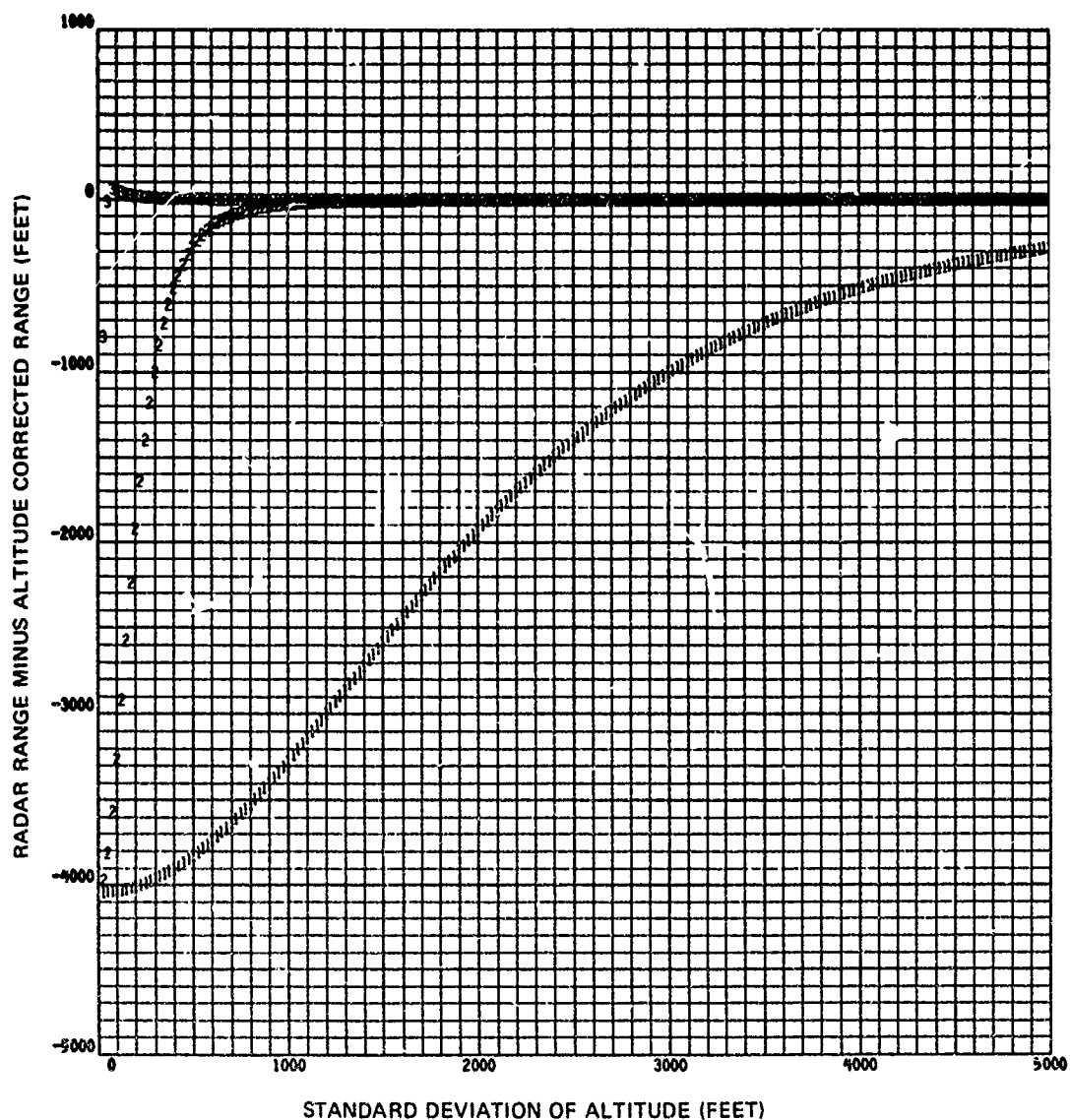
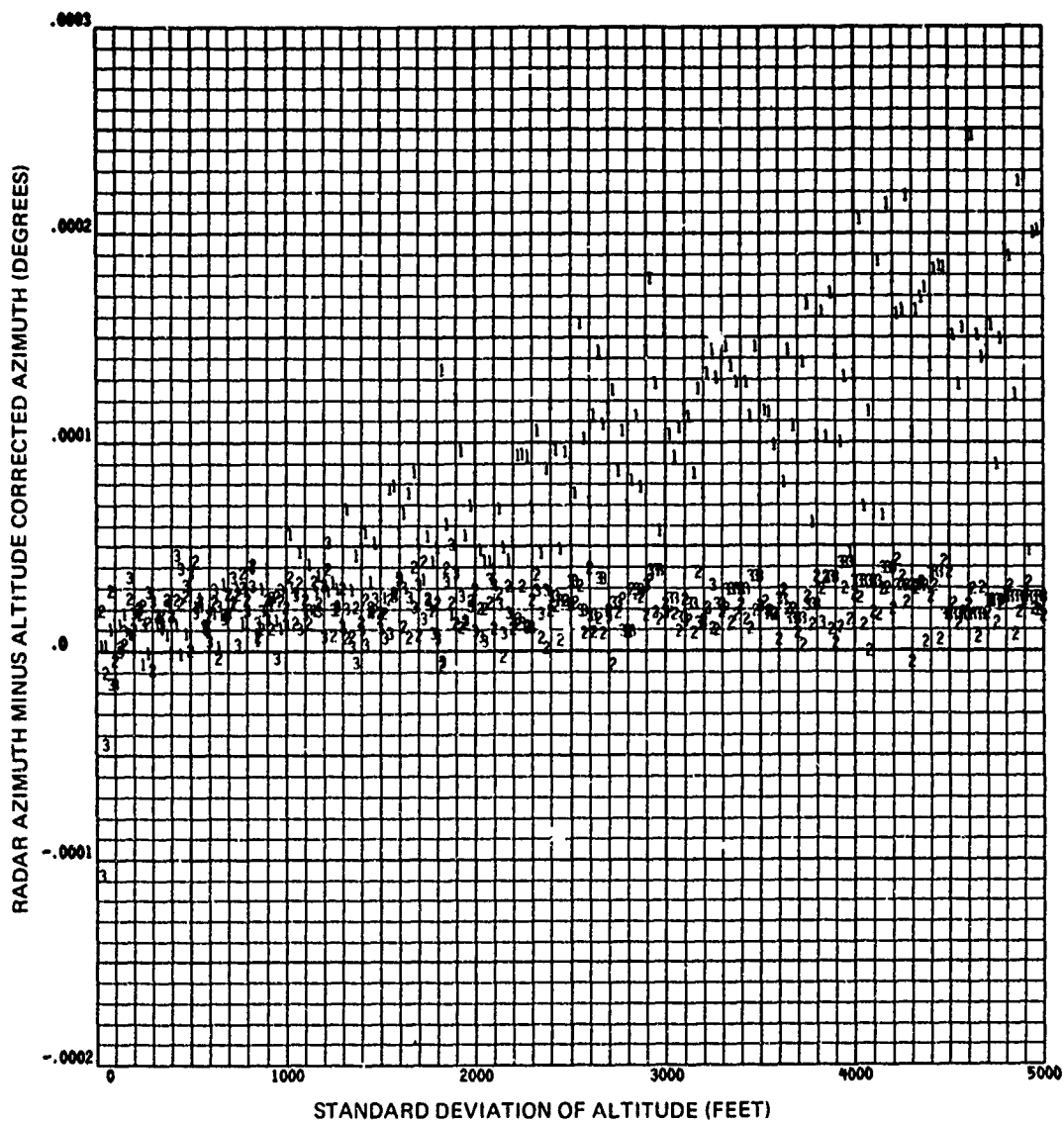


Figure 1. Example of a Geometric Situation Used to Determine Algorithm Effects and Improvement in Accuracy.



- NOTES:
1. STANDARD DEVIATIONS IN ELEVATION ARE REPRESENTED BY THE FOLLOWING SYMBOLS:
 1 -- $\sigma_E = 10$ MILS
 2 -- $\sigma_E = 1$ MIL
 3 -- $\sigma_E = 0.1$ MIL
 2. STANDARD DEVIATION IN RANGE (σ_R) IS CONSTANT AT 10 FEET.
 3. STANDARD DEVIATION IN AZIMUTH (σ_A) IS CONSTANT AT 0.1 MIL.

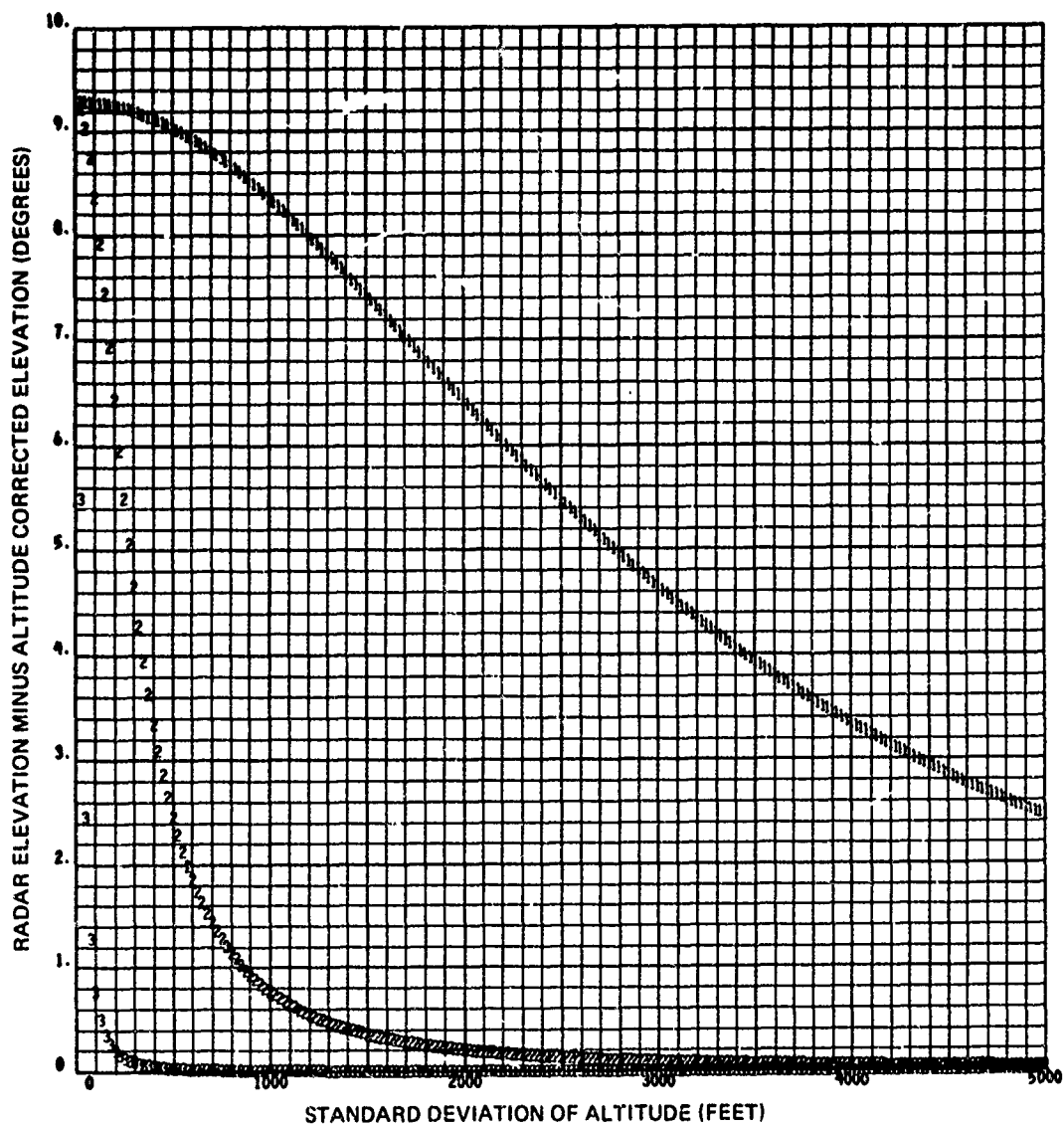
Figure 2. Plots Showing the Effects of the Algorithm With Respect to Variances in the Elevation Measurement.



- NOTES:
1. STANDARD DEVIATIONS IN ELEVATION ARE REPRESENTED BY THE FOLLOWING SYMBOLS:
 1 -- $\sigma_E = 50$ MILS
 2 -- $\sigma_E = 1$ MIL
 3 -- $\sigma_E = 0.1$ MIL
 2. STANDARD DEVIATION IN RANGE (σ_R) IS CONSTANT AT 10 FEET.
 3. STANDARD DEVIATION IN AZIMUTH (σ_A) IS CONSTANT AT 0.1 MIL.

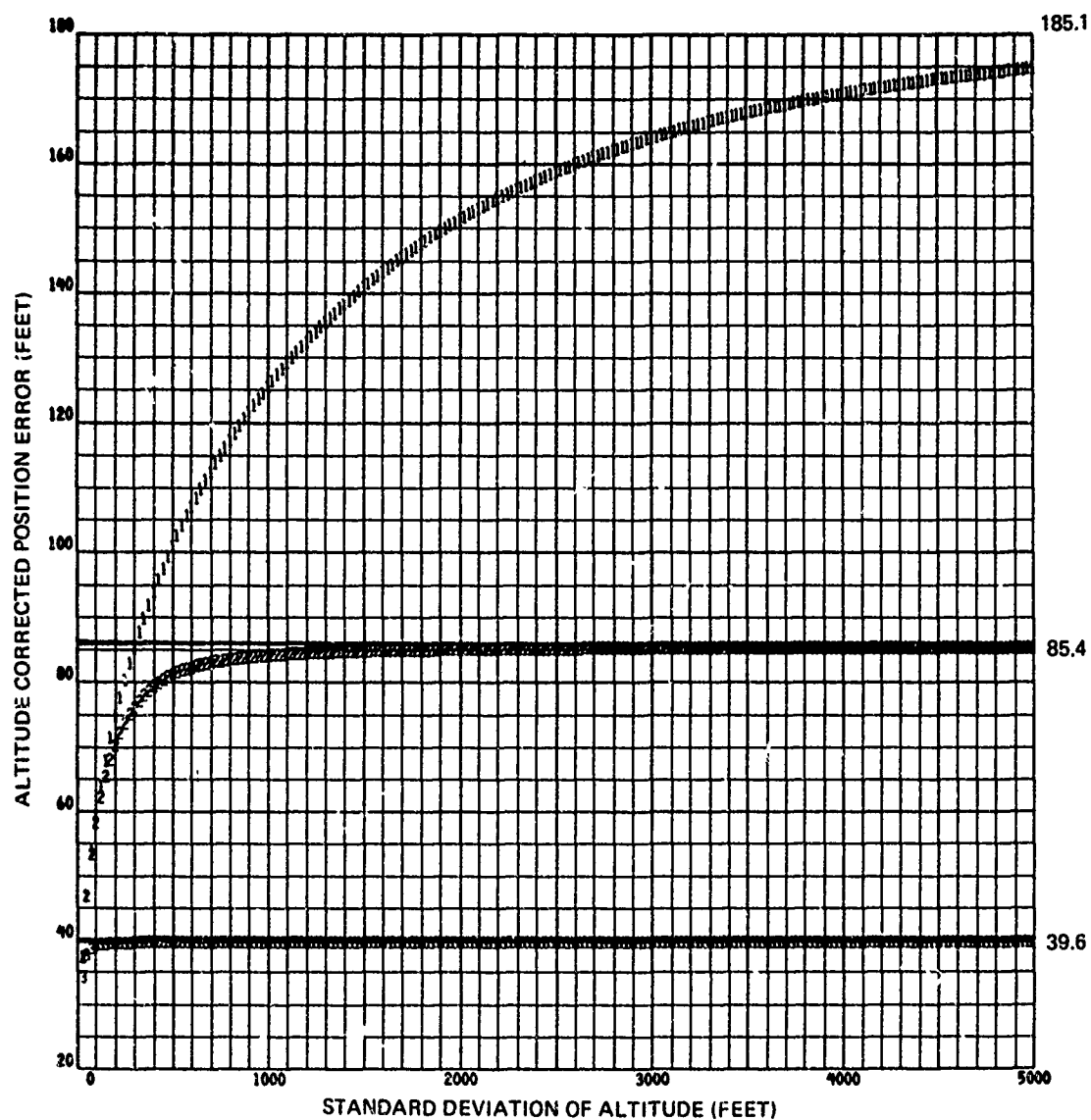
Figure 2. Continued.





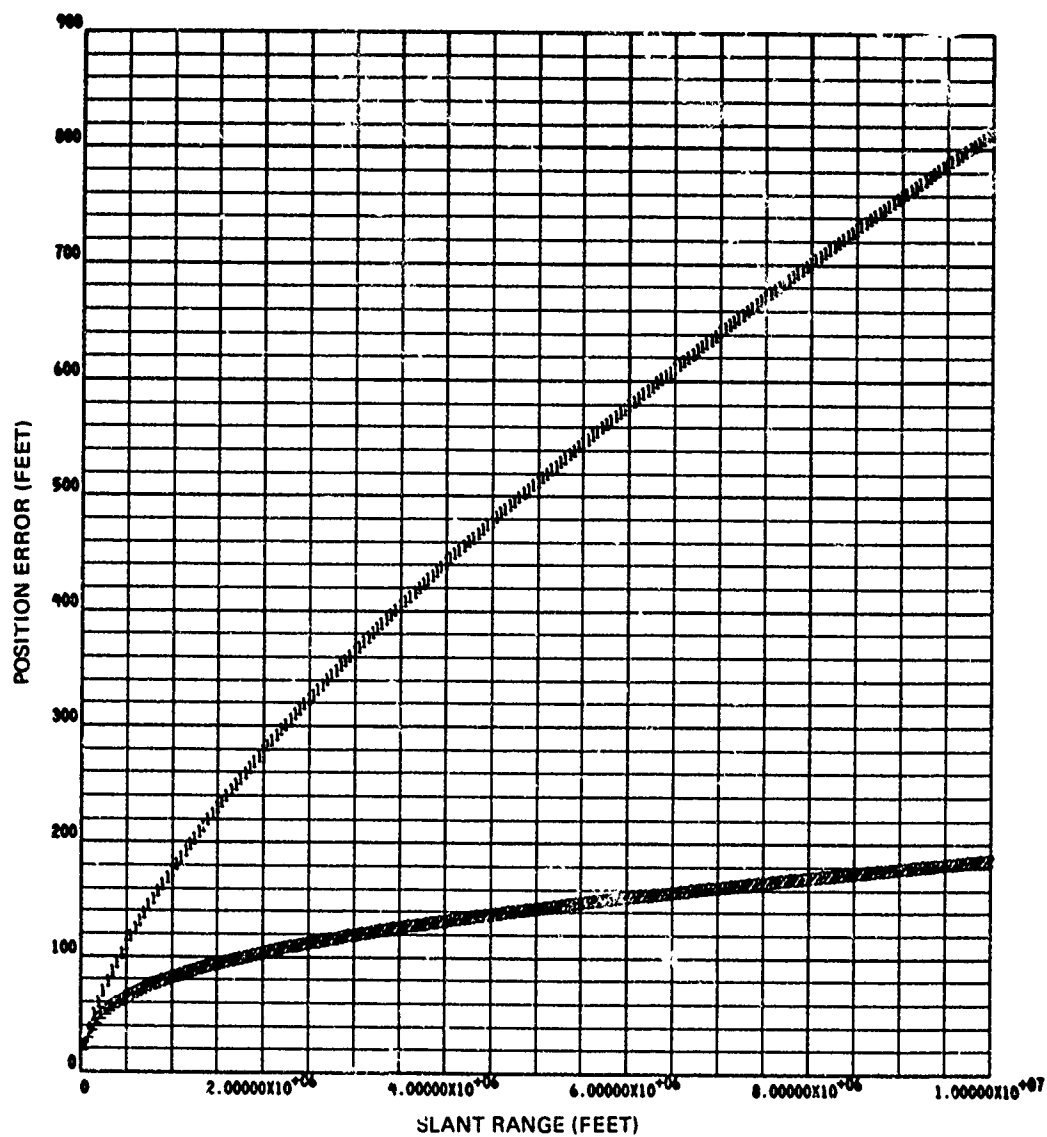
- NOTES:
1. STANDARD DEVIATIONS IN ELEVATION ARE REPRESENTED BY THE FOLLOWING SYMBOLS:
 1 -- $\sigma_E = 10$ MILS
 2 -- $\sigma_E = 1$ MIL
 3 -- $\sigma_E = 0.1$ MIL
 2. STANDARD DEVIATION IN RANGE (σ_R) IS CONSTANT AT 10 FEET.
 3. STANDARD DEVIATION IN AZIMUTH (σ_A) IS CONSTANT AT 0.1 MIL.

Figure 2. Concluded.



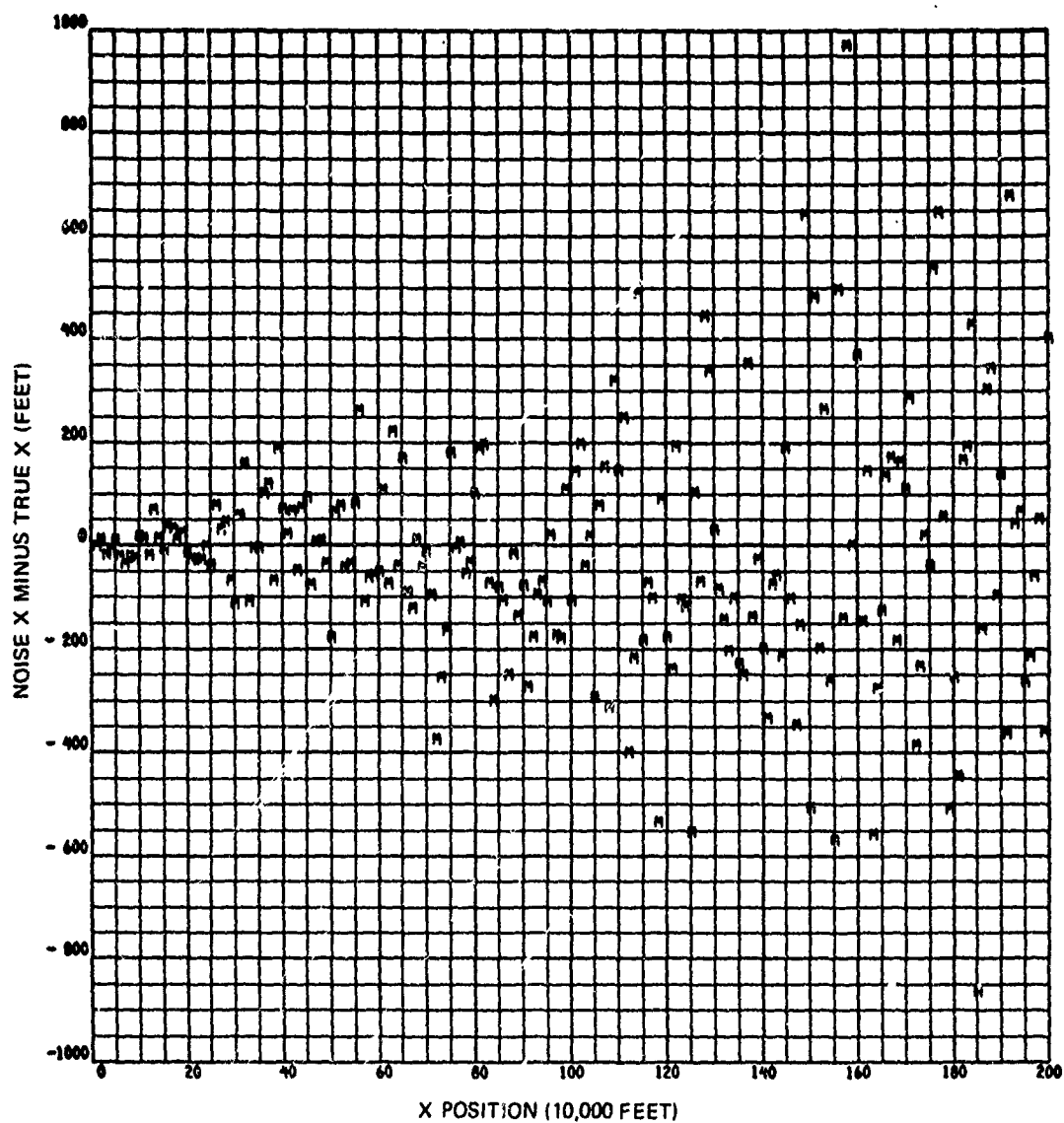
- NOTES:
1. STANDARD DEVIATIONS IN ELEVATION ARE REPRESENTED BY THE FOLLOWING SYMBOLS:
 - 1 -- $\sigma_E = 10$ MILS
 - 2 -- $\sigma_E = 1$ MIL
 - 3 -- $\sigma_E = 0.1$ MIL
 2. STANDARD DEVIATION IN RANGE (σ_R) IS CONSTANT AT 10 FEET.
 3. STANDARD DEVIATION IN AZIMUTH (σ_A) IS CONSTANT AT 0.1 MIL.

Figure 3. Plot Showing the Increase in Precision of the Algorithm Over the Radar-Only Solution.



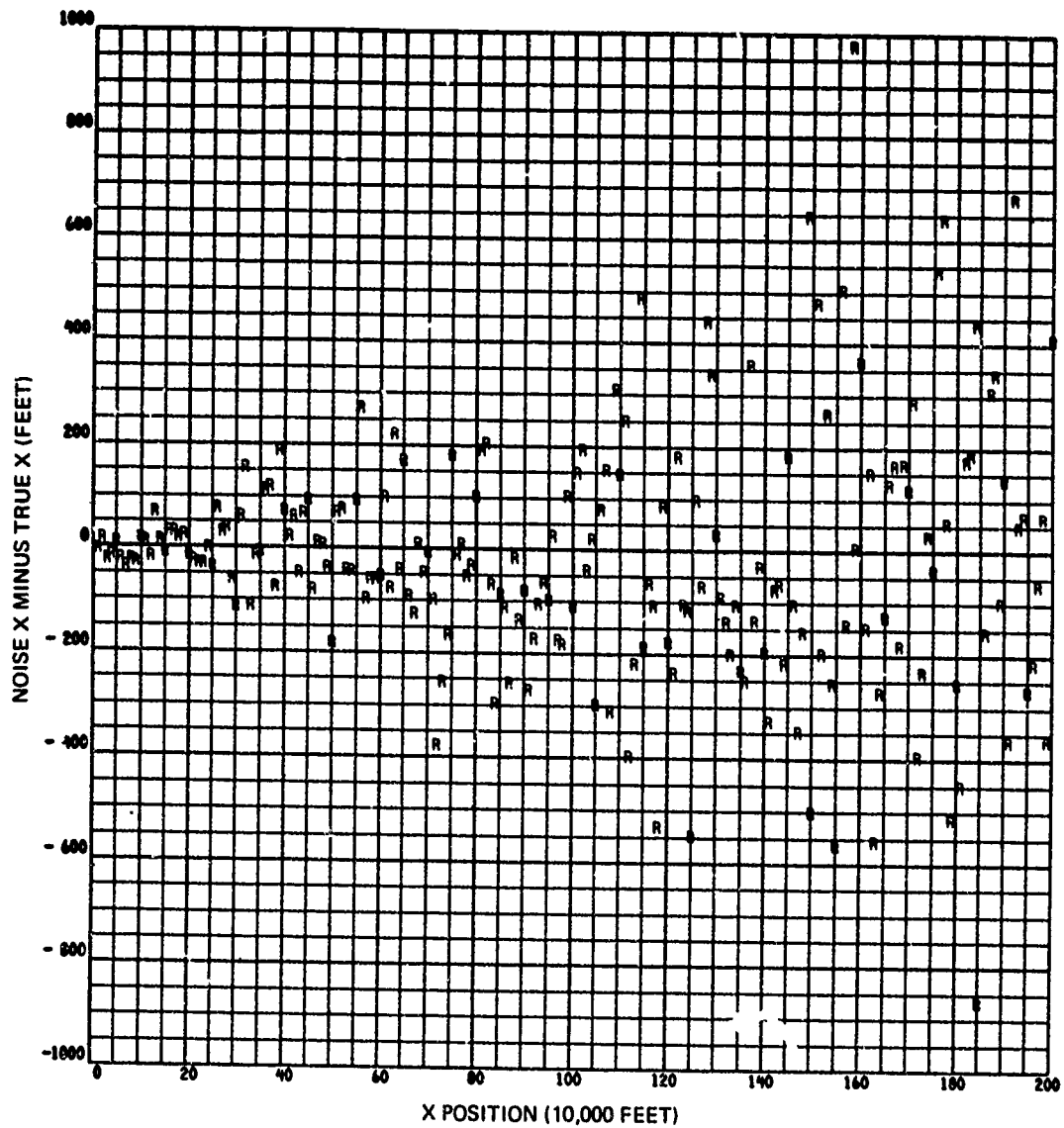
- NOTES:
1. POSITION ERRORS AS A FUNCTION OF SLANT RANGE ARE REPRESENTED BY THE FOLLOWING SYMBOLS:
 1 -- RADAR ONLY
 2 -- RADAR AND ALTITUDE
 2. STANDARD DEVIATIONS ARE THE FOLLOWING:
 RANGE -- $\sigma_R = 20$ FEET
 AZIMUTH -- $\sigma_A = 0.2$ MIL
 ELEVATION -- $\sigma_E = 0.2$ MIL
 ALTITUDE -- $\sigma_H = 20$ FEET

Figure 4. Plot Showing the Increases in Position Accuracy as Range Increases.



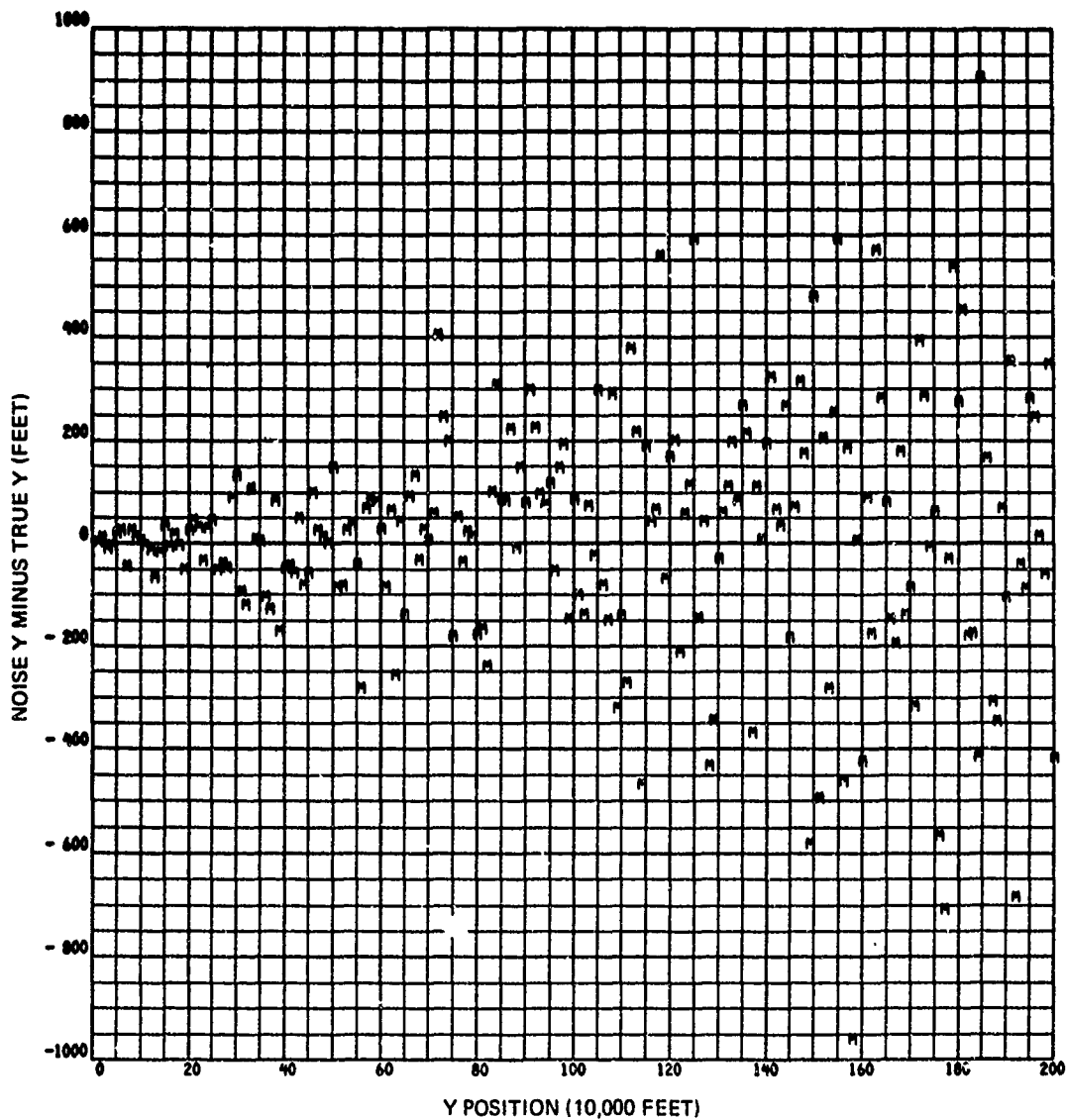
- NOTES: 1. MAXIMUM LIKELIHOOD ERROR IS REPRESENTED BY THE SYMBOL M.
2. STANDARD DEVIATIONS ARE THE FOLLOWING:
- RANGE -- $\sigma_R = 20$ FEET
 - AZIMUTH -- $\sigma_A = 0.2$ MIL
 - ELEVATION -- $\sigma_E = 0.2$ MIL
 - ALTITUDE -- $\sigma_H = 20$ FEET

Figure 5. Plots Showing the Cartesian Coordinate That the Altitude Measurement Aids.



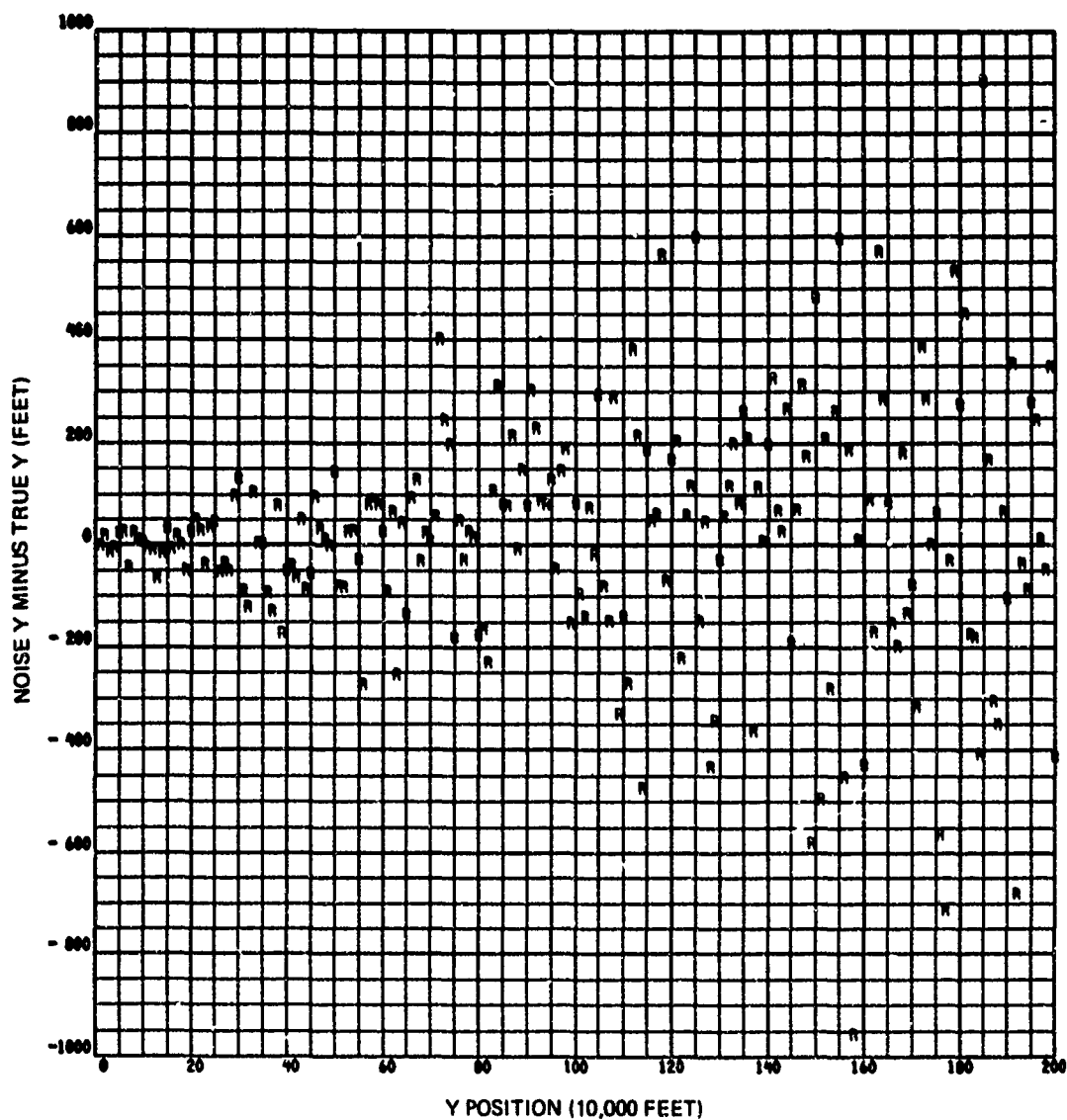
- NOTES: 1. RADAR ERROR IS REPRESENTED
BY THE SYMBOL R.
2. STANDARD DEVIATIONS ARE THE
FOLLOWING:
- RANGE -- $\sigma_R = 20$ FEET
- AZIMUTH -- $\sigma_A = 0.2$ MIL
- ELEVATION -- $\sigma_E = 0.2$ MIL

Figure 5. Continued.



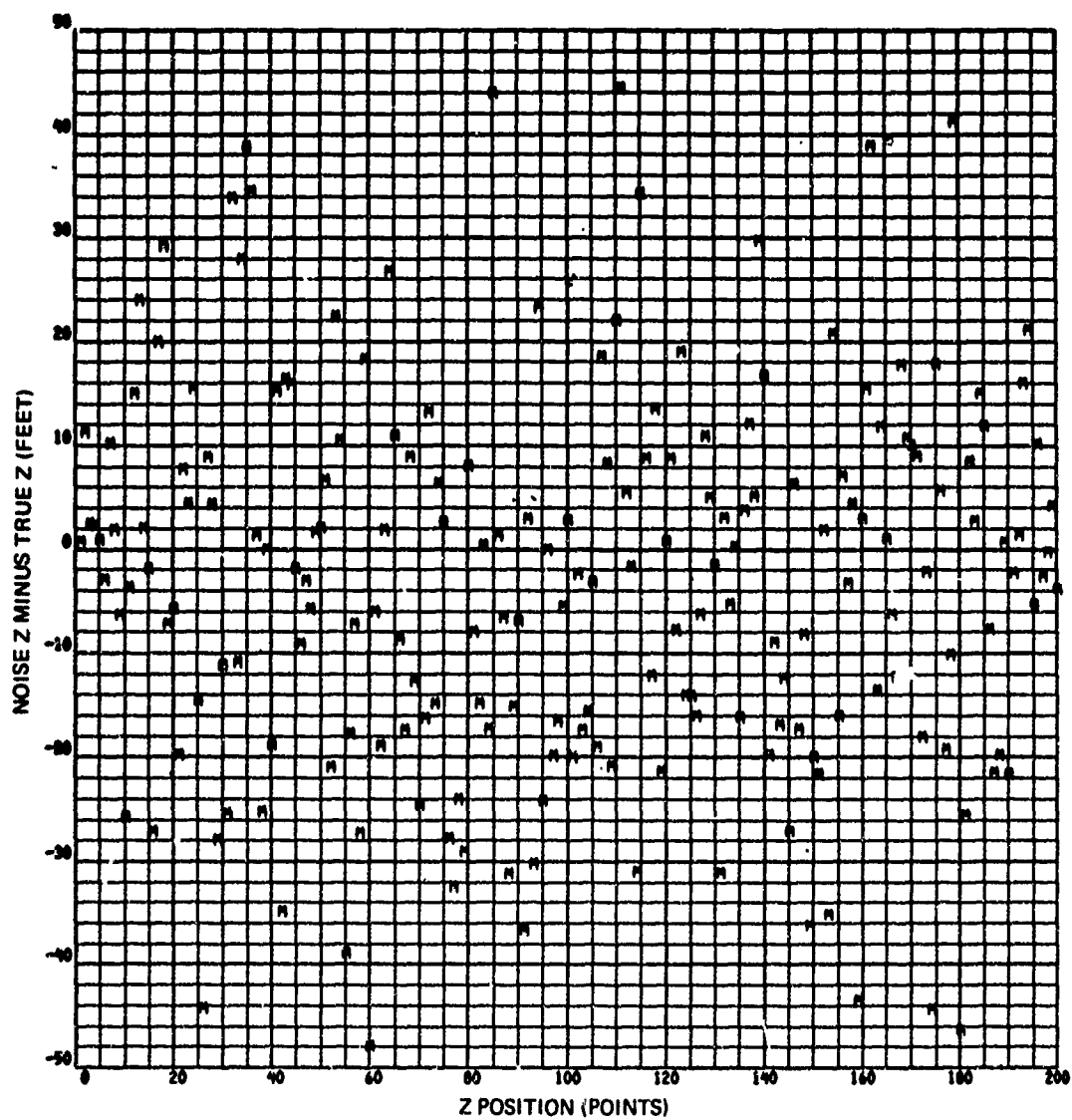
- NOTES: 1. MAXIMUM LIKELIHOOD ERROR IS REPRESENTED BY THE SYMBOL M.
2. STANDARD DEVIATIONS ARE THE FOLLOWING:
- RANGE -- $\sigma_R = 20$ FEET
- AZIMUTH -- $\sigma_A = 0.2$ MIL
- ELEVATION -- $\sigma_E = 0.2$ MIL
- ALTITUDE -- $\sigma_H = 20$ FEET

Figure 5. Continued.



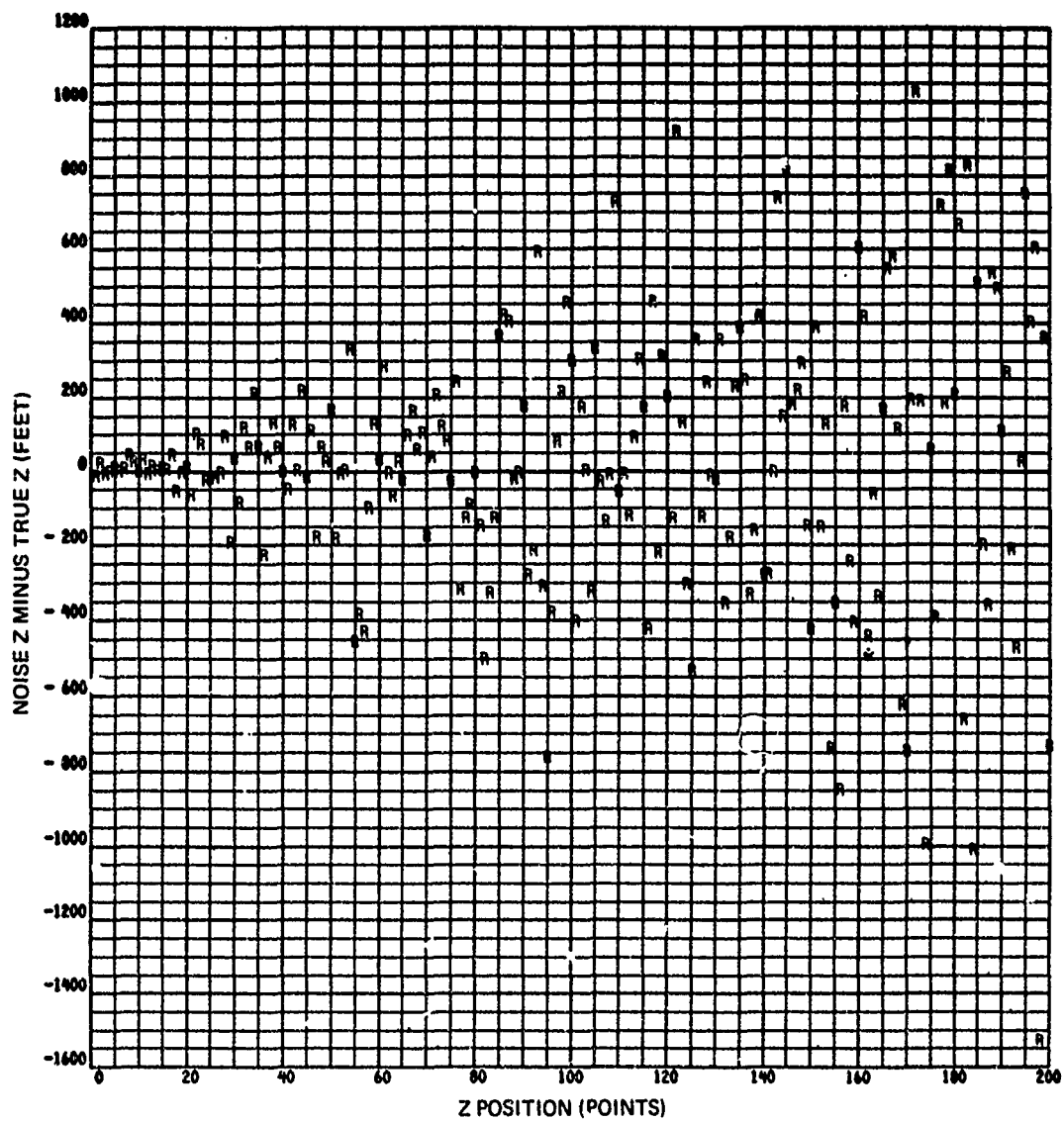
- NOTES: 1. RADAR ERROR IS REPRESENTED
BY THE SYMBOL R.
2. STANDARD DEVIATIONS ARE THE
FOLLOWING:
- RANGE -- $\sigma_R = 20$ FEET
- AZIMUTH -- $\sigma_A = 0.2$ MIL
- ELEVATION -- $\sigma_E = 0.2$ MIL

Figure 5. Continued.



- NOTES: 1. MAXIMUM LIKELIHOOD ERROR IS REPRESENTED BY THE SYMBOL M.
2. STANDARD DEVIATIONS ARE THE FOLLOWING:
- RANGE -- $\sigma_R = 20$ FEET
 - AZIMUTH -- $\sigma_A = 0.2$ MIL
 - ELEVATION -- $\sigma_E = 0.2$ MIL
 - ALTITUDE -- $\sigma_H = 20$ FEET

Figure 5. Continued.



- NOTES: 1. RADAR ERROR IS REPRESENTED BY THE SYMBOL R.
2. STANDARD DEVIATIONS ARE THE FOLLOWING:
- RANGE -- $\sigma_R = 20$ FEET
- AZIMUTH -- $\sigma_A = 0.2$ MIL
- ELEVATION -- $\sigma_E = 0.2$ MIL

Figure 5. Concluded.

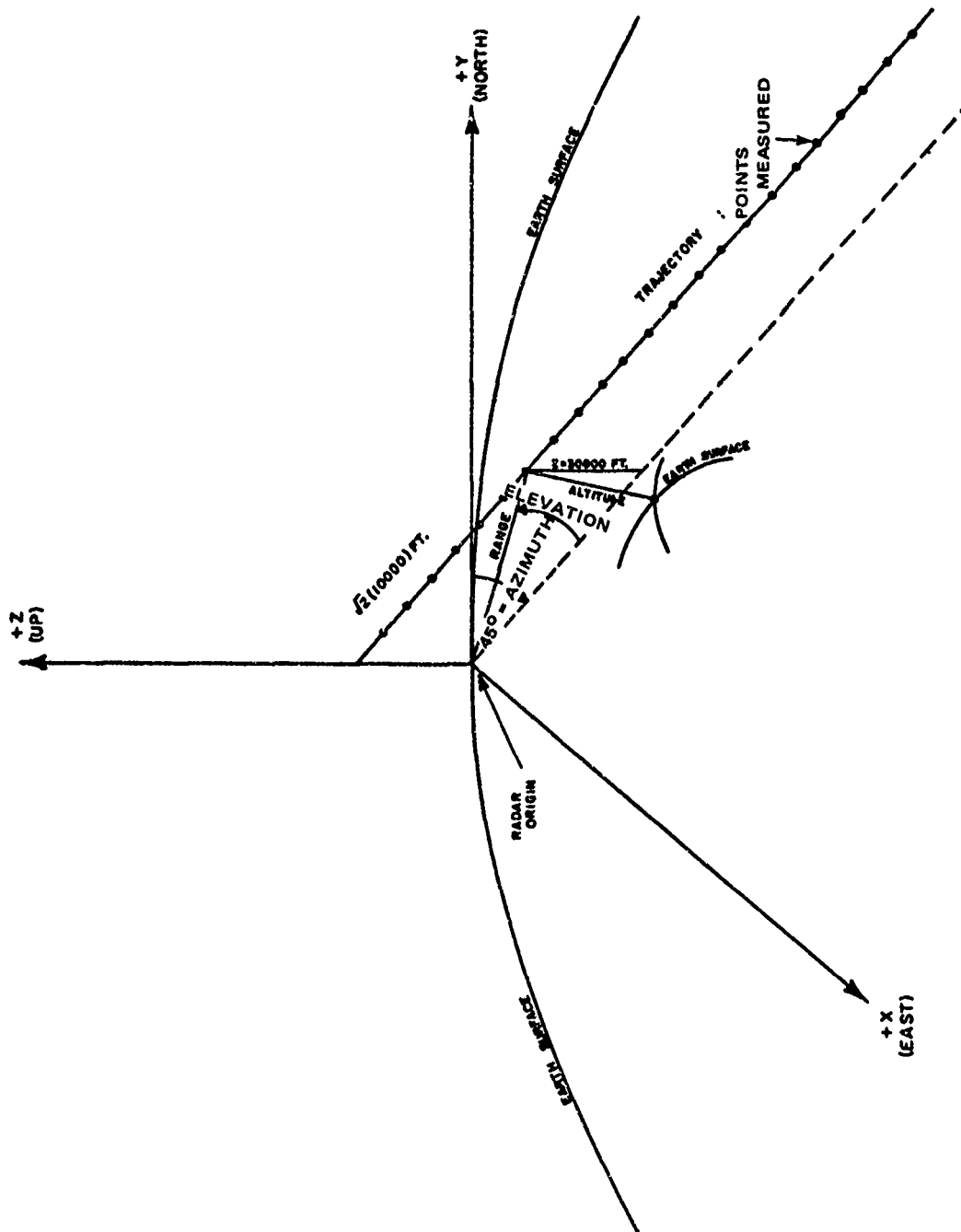
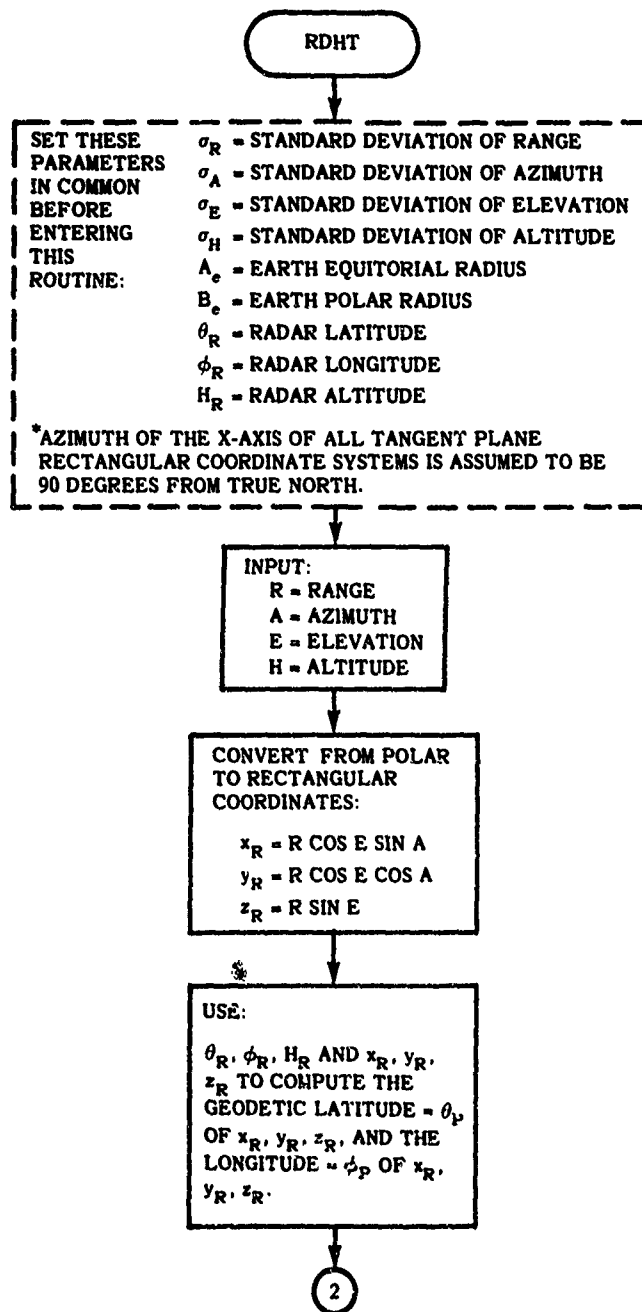


Figure 6. Example of a Geometric Situation Used to Determine Improvement in Algorithm Accuracy.

**APPENDIX
FLOWCHARTS**

Preceding page blank



2

A = MATRIX OF PARTIALS WHICH CONVERTS A POLAR COVARIANCE MATRIX TO A RECTANGULAR ONE

$$\begin{aligned} a_{11} &= \cos E \sin A \\ a_{12} &= R \cos E \cos A \\ a_{13} &= -R \sin E \sin A \\ a_{21} &= \cos E \cos A \\ a_{22} &= -R \cos E \sin A \\ a_{23} &= -R \sin E \cos A \\ a_{31} &= \sin E \\ a_{32} &= 0 \\ a_{33} &= R \cos E \end{aligned}$$

B = MATRIX WHICH CONVERTS THE RECTANGULAR COVARIANCE MATRIX IN THE RADAR SYSTEM TO A RECTANGULAR COVARIANCE MATRIX IN TANGENT PLANE SYSTEM LOCATED AT $(\theta_P, \phi_P, 0)$

$$\begin{aligned} b_{11} &= \cos(\phi_P - \phi_R) \\ b_{12} &= \sin \theta_R \sin(\phi_P - \phi_R) \\ b_{13} &= -\cos \theta_R \sin(\phi_P - \phi_R) \\ b_{21} &= -\sin \theta_P \sin(\phi_P - \phi_R) \\ b_{22} &= \cos \theta_R \cos \theta_P + \sin \theta_R \sin \theta_P \cos(\phi_P - \phi_R) \\ b_{23} &= \sin \theta_R \cos \theta_P - \cos \theta_R \sin \theta_P \cos(\phi_P - \phi_R) \\ b_{31} &= \cos \theta_P \sin(\phi_P - \phi_R) \\ b_{32} &= \cos \theta_R \sin \theta_P - \sin \theta_R \cos \theta_P \cos(\phi_P - \phi_R) \\ b_{33} &= \sin \theta_R \sin \theta_P + \cos \theta_R \cos \theta_P \cos(\phi_P - \phi_R) \end{aligned}$$

$$C_M = B A \begin{bmatrix} \sigma_R^2 & 0 & 0 \\ 0 & \sigma_A^2 & 0 \\ 0 & 0 & \sigma_E^2 \end{bmatrix} A^T B^T$$

3

